Wind and Structures, Vol. 13, No. 5 (2010) 413-431
DOI: http://dx.doi.org/10.12989/was.2010.13.5.413

Assessment of vertical wind loads on lattice framework with application to thunderstorm winds

T.G. Mara*[1], J.K. Galsworthy[2,3] and E. Savory[4]

[1]The Boundary Layer Wind Tunnel Laboratory, The University of Western Ontario, London, ON, Canada N6A 5B9
[2]Former Address: The Boundary Layer Wind Tunnel Laboratory, The University of Western Ontario, London, ON, Canada N6A 5B9
[3]Current Address: Rowan Williams Davies & Irwin Inc., 650 Woodlawn Road West, Guelph, ON, Canada, N1K 1B8
[4]Department of Mechanical and Materials Engineering, The University of Western Ontario, London, ON, Canada N6A 5B9

(Received July 21, 2009, Accepted March 3, 2010)

Abstract. The focus of this article is on the assessment of vertical wind vector components and their aerodynamic impact on lattice framework, specifically two distinct sections of a guyed transmission tower. Thunderstorm winds, notably very localized events such as convective downdrafts (including downbursts) and tornadoes, result in a different load on a tower's structural system in terms of magnitude and spatial distribution when compared to horizontal synoptic winds. Findings of previous model-scale experiments are outlined and their results considered for the development of a testing rig that allows for rotation about multiple body axes through a series of wind tunnel tests. Experimental results for the wind loads on two unique experimental models are presented and the difference in behaviour discussed. For a model cross arm with a solidity ratio of approximately 30%, the drag load was increased by 14% when at a pitch angle of 20º. Although the effects of rotation about the vertical body axis, or the traditional 'angle of attack', are recognized by design codes as being significant, provisions for vertical winds are absent from each set of wind loading specifications examined. The inclusion of a factor to relate winds with a vertical component to the horizontal speed is evaluated as a vertical wind factor applicable to load calculations. Member complexity and asymmetric geometry often complicate the use of lattice wind loading provisions, which is a challenge that extends to future studies and codification. Nevertheless, the present work is intended to establish a basis for such studies.

Keywords: lattice tower; wind tunnel testing; thunderstorm winds; non-horizontal wind; downburst simulation; transmission tower.

1. Introduction

Most wind-related failures of transmission lines worldwide can be attributed to high intensity, small-scale events (Dempsey and White 1996, Nolasco 1996, Li 2000), such as thunderstorm winds and associated convective downdrafts (including downbursts) and tornadoes. While thunderstorm

* Corresponding Author, Project Engineer, E-mail: tmara3@uwo.ca

wind events may be small in size compared to strong synoptic wind events, they especially pose a threat to electrical transmission systems due to the large spatial coverage of the networks of towers and conductors. The wind loading conditions during a thunderstorm wind event differ from those of synoptic wind loading in a number of ways:

1. The vertical profile of a thunderstorm gust front or downburst is significantly different in shape to traditional atmospheric boundary layer winds (Letchford *et al*. 2002) and can have very strong winds close to ground level. In the case of a downburst, this is due to the convective downdraft impinging on the ground and propagating radially outward, a model that has showed reasonable agreement with full scale data (Wood *et al.* 2001). For gust fronts, high wind speeds can arise due to local convection as well as translation of the storm cell. An empirical model of a downburst is presented by Holmes and Oliver (2000) in which the wind profile accounts for a translating component as well. This was shown to have good agreement in wind speed and direction compared to full-scale data recorded during an downburst event at Andrews Air Force Base in 1983 (Fujita 1985). The influence of the angle of impingement of a downburst is discussed by Mason *et al.* (2009), and it is shown that 'tilted' downbursts have the potential of creating even more extreme structural loading conditions than those impinging normal to the ground.
2. The resultant wind vector is characterized by a significant vertical component (Hangan *et al.* 2003) which increases the wind loading on lattice structures. From examination of the CFD data of this simulation, the vertical component at the point of maximum horizontal outflow velocity was found to be in the range of 20%. This ratio can be much more severe in the case of tornadoes. In a simulation (Savory *et al.* 2001) of a tornado passing a transmission tower, the maximum horizontal wind speeds were found to be approximately 115 m/s while the simultaneous vertical winds were found to be approximately 75 m/s.

The combination of these wind field characteristics result in a structural loading situation which is not considered in any wind design codes. Certain codes for overhead lines (ASCE 1991, Standards Australia 2003) specify increased wind loads for convective downdrafts and tornadoes, although the increase is applied as a higher horizontal wind speed and therefore does not impact loading in the vertical direction. Structural failure is often the result of the extreme conditions presented by thunderstorm winds, the impetus of the current research being an example. In September 1996, a series of thunderstorm winds spawned many convective wind events in southern Manitoba, Canada. As a result, 19 consecutive towers experienced failure in a vital part of the Manitoba Hydro power grid leaving some serviced areas without power for up to five days. In a forensic report, McCarthy and Melsness (1996), it was concluded that the tower failures were most likely due to high winds resulting from multiple downburst events. These failures led to the present project to better understand the interaction of thunderstorm gust front, convective downdraft and tornadic winds with a typical guyed lattice tower (see Savory *et al.* 2008). When designing line systems utility companies examine a range of load cases, including the wind and ice load combined and broken conductor cases, in order to identify the critical loads for a particular design. For these cases, which consider regular synoptic winds, the key wind direction is perpendicular to the line and, hence, parallel to the cross-arms of the tower. However, it has been shown (Shehata and El Damatty 2007, 2008) from finite element analyses of the effects of downburst winds on guyed towers, that the critical cases are mostly where the event impacts asymmetrically with respect to the tower location such that the cross-arms are impacted by the downburst outflow.

Although the underlying meteorological process for various types of convective wind events can be very different, the gust front structure can be similar in terms of profile shape and strength, which is advantageous when considering their interaction with structures. While the small scales typically used for computational downburst modelling, ranging from 1:3000 to 1:25 000 (Chay *et al.* 2006, Kim and Hangan 2007), have hindered their application to physical models, the results from numerical simulations have been applied analytically to numerical structural models. Examples of these include the application to a structural model of a free-standing tower by Savory *et al.* (2001), a guyed tower by Shehata and El Damatty (2007), and the application to tall buildings by Chen and Letchford (2004) and Kim *et al.* (2007). The results of downburst modelling are extended to risk assessment and hazard studies for transmission line networks in Oliver *et al.* (2000). However, in the case of the most relevant work to the current study by Shehata and El Damatty (2007), the loading and shielding coefficients (NBCC 2005) which were used are based on horizontal winds and carry a disclaimer regarding their accuracy (due to testing parameters). In a significant step forward in physical modelling, a large-scale downburst outflow testing facility has recently been installed at the Boundary Layer Wind Tunnel Laboratory, which has the capacity of applying transient downburst loading to models at scales of the order of 1:400 (Lin *et al*. 2007). While wind field models have been applied analytically, assessment of the implications of vertical wind components on lattice section design has not previously been investigated.

Wind loads on lattice sections are sensitive to wind direction due to aerodynamic properties such as shielding and projected frontal area, which can vary significantly over small angles of adjustment in orientation. In the case of thunderstorm gust front or downburst outflow, where the wind field is shown to possess a substantial vertical component (Fujita 1990, Hangan *et al.* 2003, Ponte Jr. and Riera 2007), increases in the wind loading of lattice sections can arise from two processes which differ from purely horizontal wind cases.

The first increase is due to the wind field of the thunderstorm gust front or downburst. The vertical component causes an increase in the resultant wind speed based on the angle of inclination with respect to the horizontal. This is important for design and codification purposes because both measured and code-specified wind speeds are referenced to horizontal wind speeds. The rear flank downdraft documented by Orwig and Schroeder (2007) measured a peak horizontal speed of 39 m/s, which is within 1 m/s of the 50-year ASCE design wind speed specified for the area. This event is examined in detail by Holmes *et al*. (2008) and shows that the lateral correlations are high compared to those for synoptic winds, which brings into question the use of conventional span reduction factors for downburst or thunderstorm gust front winds.

The second increase is due to the aerodynamic properties of the section as it rotates about various axes. Most wind loading codes recognize the difference in wind loading from different azimuths, but this is rotation about a single vertical axis commonly referred to as the yaw axis. As demonstrated in this paper, rotations about an additional body axis, referred to as the pitch axis, can also produce increased loads for some lattice geometries. This is attributed to the complex member geometry and the effects that rotation has on the values of projected area and the shielding coefficient. In this paper, the values for this increase are section specific, but advice is offered as to which types of geometries are sensitive to increases in loading due to pitch rotation, which is analogous to wind flow with a vertical component. A convenient method of representing this increase is a factor which can be written as a ratio of the nominal effective projected area and directly applied with the specified dynamic pressure.

By combining the increase in wind speed due to a vertical wind component with the increase due to varying aerodynamic section effects, the resulting wind loads on a lattice structure could be significantly greater than those recommended in code provisions. The factors presented in this paper are directly applicable to the calculation of quasi-steady mean loads. It should be noted that these provide an upper bound and, in the interest of financial feasibility, should be considered with the inclusion of some measure of probability or a risk assessment study. It should also be noted that when considering vertical wind loads associated with thunderstorm gust front or downburst wind loading, the cross-arm is a vulnerable part of the tower. As cross-arms are designed to support the loads due to gravity of the conductors (including ice load) they may contain members that are designed for zero axial loading. The net result of an upwards or downwards vertical load due to inclined winds may induce compression forces in those members that are not accounted for in design. The scope of the current discussion is limited to the components which contribute to the vertical loading, rather than the overall effects on the complete structure.

The following section discusses previous work concerning experimental measurement of wind loads on lattice sections, which emphasizes the lack of data for non-horizontal winds. This is followed by details of the models tested in the present study, together with a unique testing rig that allowed for models to be tested with rotations about multiple body axes. Results of the wind tunnel tests are then presented for each model, with the focus of the discussion being on the effects of their geometry and solidity ratio. Finally, a method of accounting for increases due to non-horizontal winds through the use of a loading factor is presented.

2. Lattice tower testing

Due to the challenges posed by reduced scale experimentation on lattice sections, primarily due to the physical size of the members, there is a dearth of wind tunnel test data available when compared to other common structures. In the past, experiments have used scales ranging 1:8 to 1:50, at which it is challenging to properly construct wind tunnel models. The current work is limited to experimental work involving static models of lattice sections.

The investigations of wind effects on trusses conducted by Flachsbart and Winter (1934) to determine the effect of varying angle of attack and shielding phenomena has served as a springboard into further studies on trusses, arrays of lattice frames, and 3-dimensional lattice structures. It was through these experiments that empirical relationships between wake velocities and resulting frame drag coefficients were originally drawn. The importance of the solidity ratio to the drag coefficient was expressed by Pagon (1958), and resulted in drag coefficient estimates for single trusses which were specified in the ANSI Standard until 1982 (ANSI 1982). However, much of the design work involving lattice structures continued on a case-by-case basis. Later studies by Sykes (1981) and Bayar (1986) exhibited drag coefficient relationships consistent with Pagon's work, but only over limited solidity ranges.

While Flachsbart (1932) and Pagon (1958) focused on a single truss, many lattice structures comprise a pair of trusses connected by lateral members, typically referred to as a 3-dimensional frame. This design introduces the effect of shielding; the impact that the upwind frame has on the airflow that acts on the downwind frame. Jacobs (1978) found that wind loading codes did not consistently reflect the varying nature of shielding with upwind frame orientation. Similar investigations were carried out by Georgiou and Vickery (1979) and Whitbread (1979) with the application of shielding to building frames which, again, revealed loading inconsistencies in the National Building Code of Canada (1977) and British Code (CP3) (1972).

The most applicable study to the present work was completed by Bayar (1986) and resulted in relationships of the drag coefficient with solidity ratio for 3-dimensional lattice frames. The equations proposed by Bayar continue to serve as the recommendations for drag coefficient values in the current Australian Standard AS/NZS 1170.2:2002 (Standards Australia 2002) and are similar to those found in ASCE Manual No. 74 (1991) to be applied with horizontal winds. Experiments using the same models rotated by up to 15° in pitch resulted in a mere 3-5% increase in measured drag coefficient, which could be due to fluctuations in the horizontal wind alone. In addition, Bayar's models were not of uniform cross-section, which could skew the extraction of a consistent drag coefficient. This is the sole reference found involving lattice structures being tested at inclined angles or for non-horizontal winds and no specification of vertical wind effects result from that.

The following section explains the wind tunnel tests that were completed as part of the present work in order to assess the effects of non-horizontal winds on lattice sections, with the focus of the test program being on model orientations pertinent to the wind fields of thunderstorm gust front or downburst outflow.

3. Experimental approach and results

3.1 Manitoba Hydro transmission tower section models

Two unique cross-sections, representing the geometry of the main conductor support arm (Model A) and typical vertical tower (Model B) of a Manitoba Hydro Type A HVDC guyed electrical transmission tower, were used as prototype for this study. The location of each of the section geometries on the prototype tower is shown in Fig. 1. The models were constructed from angled brass at a scale of 1:10, in order to meet the physical constraints of the wind tunnel, and cross-section widths varied from 5.5 mm to 9.5 mm. All member connections were soldered and rigid. Plan and elevation views of the models and their normalizing dimensions are shown in Fig. 2 and Table 1, respectively. The solidity ratios for winds at a nominal yaw angle of 0° for Models A and B

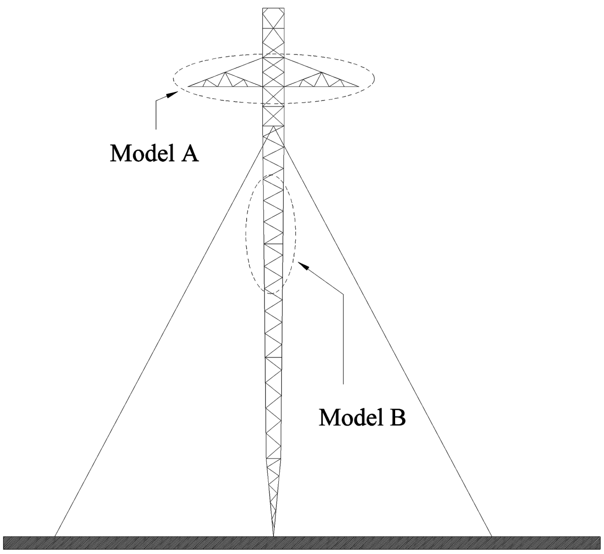

Fig. 1 Manitoba Hydro Type A tower

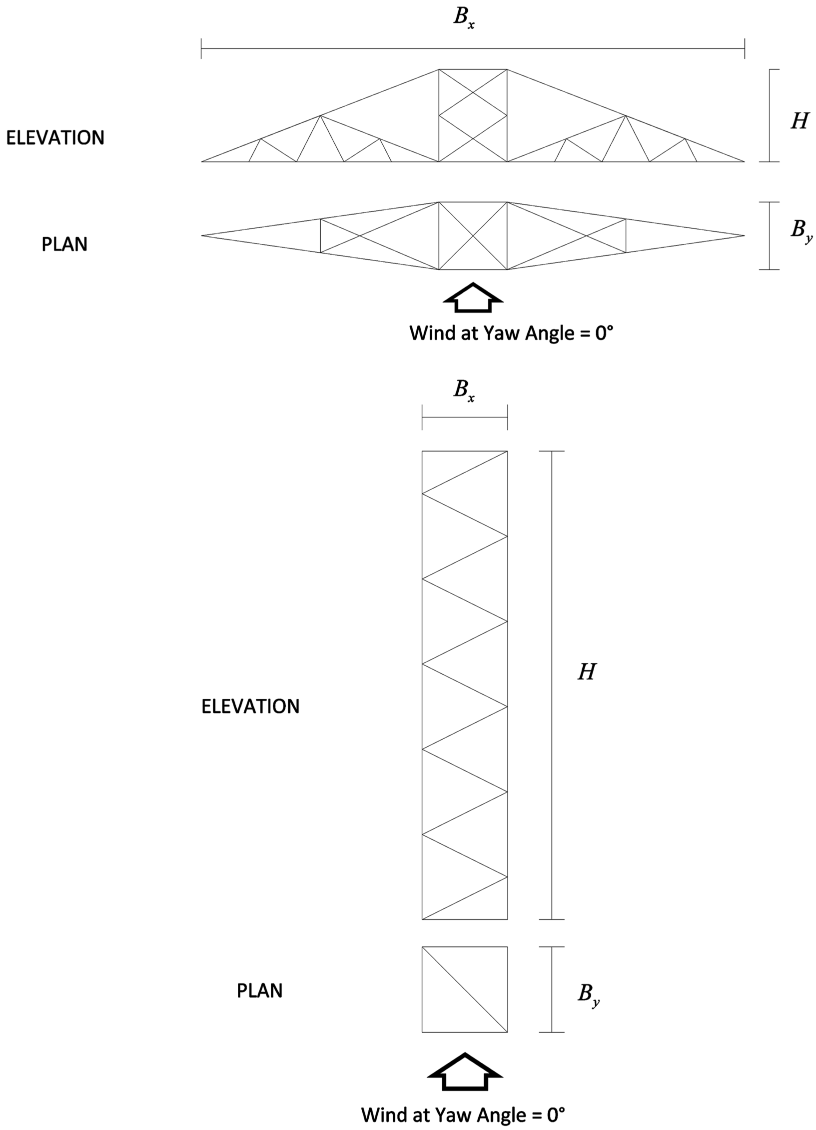

Fig. 2 Model A and B normalizing dimensions

Table 1 Model A and B normalizing dimensions

Parameter	Notation	Model A	Model B
Normalizing x-dimension (m)	B_x	0.754	0.168
Normalizing y-dimension (m)	B_y	0.168	0.168
Normalizing z-dimension (m)	H	0.168	1.003
x-face solidity	ϕ_x	0.30	0.16
y-face solidity	ϕ_y	0.22	0.18

were approximately 30% and 18%, respectively, and it should be noted that these solidity ratios serve as key design parameters used by most codes.

Aerodynamic terminology is used for the rotation of the models about their body axes, with the current focus on pitch (θ) and yaw (ψ). The axes are shown referenced to Models A and B in Fig. 3. The current experiment utilized a support strut, shielded by an aerodynamic shroud, with two joints at the top acting as a clevis. Thus, adjustment to each body axis could be made independently. Fig. 4 shows Model A in the wind tunnel at pitch angles 0º, 10º and 20º while at a yaw angle of 45º. Fig. 5 shows the same angular configurations for Model B.

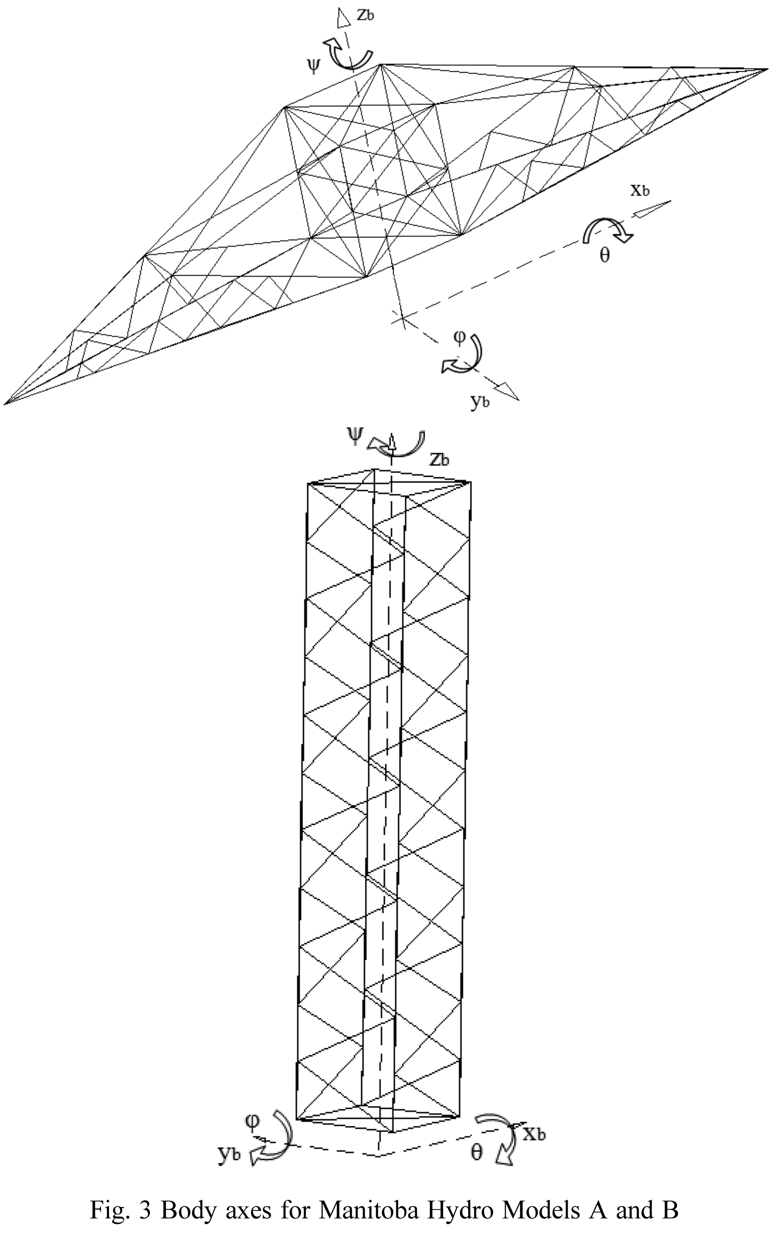

Fig. 3 Body axes for Manitoba Hydro Models A and B

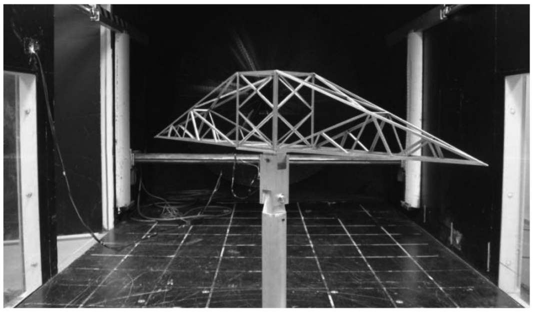

Fig. 4(a) Model A at Yaw = 45º, Pitch = 0º

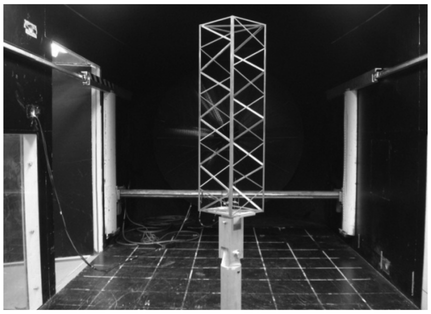

Fig. 5(a) Model B at Yaw = 45º, Pitch = 0º

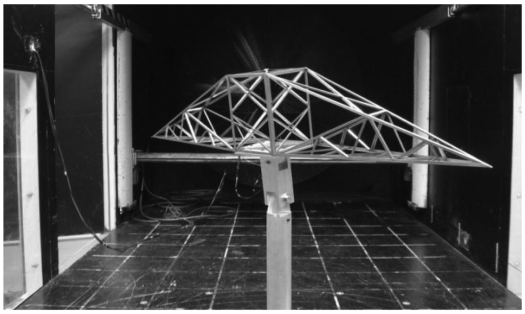

Fig. 4(b) Model A at Yaw = 45º, Pitch = 10º

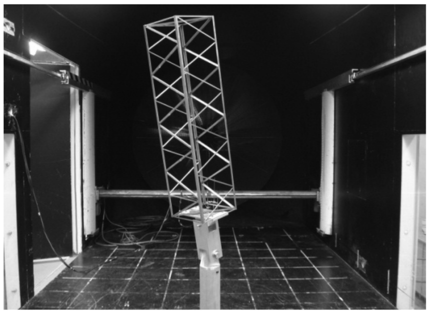

Fig. 5(b) Model B at Yaw = 45º, Pitch = 10º

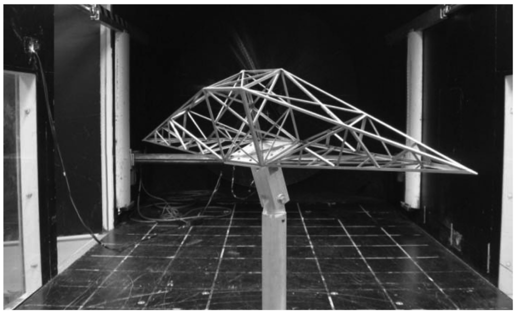

Fig. 4(c) Model A at Yaw = 45º, Pitch = 20º

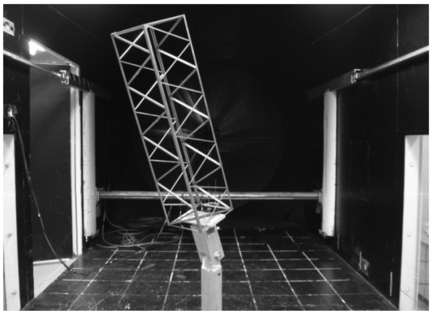

Fig. 5(c) Model B at Yaw = 45º, Pitch = 20º

3.2 Wind tunnel testing technique

The wind tunnel tests were carried out in Tunnel 1 at the Boundary Layer Wind Tunnel Laboratory at the University of Western Ontario. The dimensions of the tunnel at the test section are 2.4 m by 2.1 m in width and height, respectively. All tests were conducted in steady-state flow conditions.

Wind profiles in the horizontal and vertical directions which were uniform over the dimensions of the models were established, allowing the assumption of a quasi-steady wind pressure. All tests were carried out for a wind velocity of 7.6 m/s which was selected to provide an appropriate signal level for the measurement instrumentation being used. This resulted in a Reynolds number of approximately 4×10^3 for the data presented, although a range of Reynolds numbers between 2.3×10^3 to 6.9×10^3 were investigated. This range is consistent with that of Bayar (1986) and Sykes (1981). Although this is low relative to the prototype wind speed and dimensions, this was not seen as an issue due to the proximity and interference of adjacent members. Results from a range of wind speeds carried out for each model showed that the measurements were independent of Reynolds number, which is consistent with the general characteristics of flow past sharp-edged bodies. Tests completed for a similar lattice frame (Carril *et al.* 2003) also suggested a negligible influence of Reynolds number on mean loading. The turbulence intensity was approximately 7%, which was selected to be in the order of previous studies (Sykes 1981, Bayar 1986, Carril *et al.* 2003). However, initial configurations were also tested in a smooth flow (turbulence intensity ≈ 1%) and the effects of turbulence on the mean loads were found to be negligible, as shown by past experiments (Sykes 1981, Bayar 1986, Carril *et al.* 2003).

The wind load on the support strut alone was measured several times and found to have a maximum variation of +/-2%. The wind load on the strut alone was approximately 20% of that measured with the model in place. It was therefore treated as a tare subtraction from the measurement for each test. The effects of support interference were found to be negligible and the total model blockage was less then 5%, therefore no corrections were warranted. Both models were considered static and experienced no discernable motion during the experiments.

Non-horizontal winds were simulated by adjusting the angle of the models while maintaining horizontal wind tunnel flow. By this notion, the response of a horizontal body in inclined winds is the same as that of an inclined body in horizontal winds. The mean forces on the models were measured for a series of yaw and pitch angles, which would give the variation of the drag force with combinations of these wind angles. A complete range of yaw angles from -90° to 90°, at 10° intervals, were tested for each pitch angle. The choice of pitch angles was based on a CFD simulation of a stationary impinging jet downburst outflow modelled by Hangan *et al.* (2003). The time histories of the downburst outflow were made available to the authors and served to identify points of interest in the touchdown and gust front propagation stages of a downburst event. This simulation is presented in its entirety by Kim and Hangan (2007). From the simulation, the angle representing the resultant wind vector is treated as the pitch angle. However examination of the resultant wind field suggests an upper limit of approximately 20° to the horizontal, which is adopted as the upper limit of pitch angle for the current work. Adjustments to the pitch axis were made in 2° increments.

3.3 Experimental results

The goal of the experimental testing was to assess the variation in the aerodynamic behaviour of lattice sections as they were rotated about multiple body axes. Due to the complex geometry of lattice sections, a variety of methods exist regarding their aerodynamic description. Some codes and standards (NBCC 2005, AS/NZS 1170.2:2002) assume a constant frontal area, the nominal net area at a yaw angle of 0°, and apply a drag coefficient which varies with yaw angle. Conversely, a constant drag coefficient can be applied to a projected area which varies with yaw angle; this method necessitates the development of a 3-dimensional geometry-specific model and is, therefore, not employed by codes. ASCE Manual No. 74 (1991) decomposes forces into longitudinal and transverse components for varying yaw angle, but uses the solid frontal area of each face calculated at a yaw angle of 0° with the force coefficients given as a function of solidity ratio. The ANSI/TIA-

222-G (2006), has combined the drag coefficient and the solid projected area into a single term, carrying the units of length^2, for design requirements. This parameter is commonly referred to as Effective Projected Area (EPA). The experimental results presented in this paper are consistent with the EPA convention, as the drag force was measured at each configuration of pitch and yaw for each model. This allowed the drag measurements to be normalized by a quasi-steady dynamic pressure, yielding the term C_DA_p. This parameter facilitates the comparison of different configurations, as the effects of the changes in area are inherently included in the measurement.

The experimental results are presented in terms of model-scale C_DA_p for Model A in Figs. 6 and 7, and for Model B in Fig. 8. The results in Fig. 6 show that for Model A, the influence of pitch on the C_DA_p increases to a maximum when the frontal area is the greatest. As the shielding provided by upwind members is reduced as the pitch angle is increased, the angle with the greatest increase is a yaw angle of 0°. This relationship makes practical sense, and is important from a design standpoint as the 0° wind azimuth is the design case in many codes. The value derived from the NBCC 2005 is shown, but should be viewed as an approximation as the existing provisions are not applicable to cross-arm geometries as they have two very different faces. Fig. 7 illustrates the effect that pitch has on the C_DA_p of a lattice section based on the yaw angle of the wind. The largest variation occurs when the yaw angle is 0°, where the difference in C_DA_p between pitch angles of 0° and 20° is approximately 14%. Of interest is the fact that the greatest effect of pitch is observed at the greatest projected area, establishing the notion that if this were to be accounted for in design, then the face with the greatest projected area should be the design case. A linear relationship is shown for the range of pitch angles from 6° to 20°, however application to other cross-arm geometries is cautioned as the drag response of lattice frames is highly dependent on member shape, size and location. The effects of pitch are negligible for yaw angles 60° and 90°.

The results for Model B are plotted in Fig. 8 and exhibit a different trend in that pitch has a negligible effect on this type of section. The lack of sensitivity to pitch angle can be attributed to

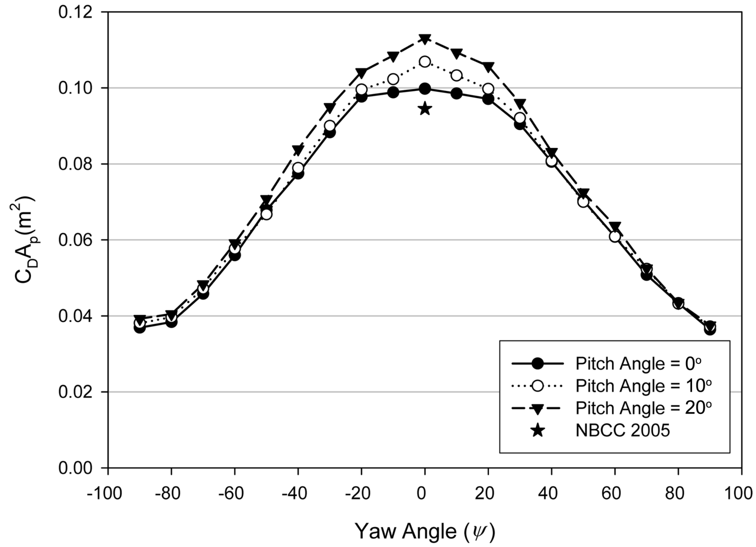

Fig. 6 Combined drag coefficient and projected frontal area, C_DA_p, vs. yaw angle for different pitch angles – Model A

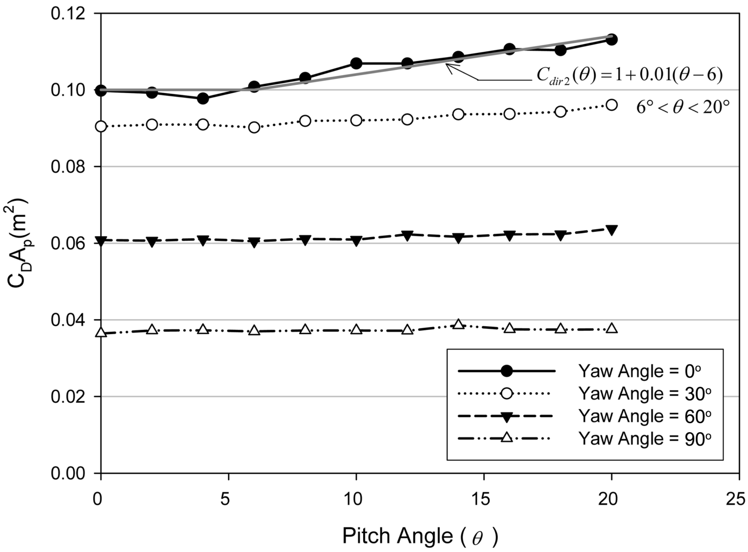

Fig. 7 Combined drag coefficient and projected frontal area, C_DA_p, vs. pitch angle for different yaw angles – Model A

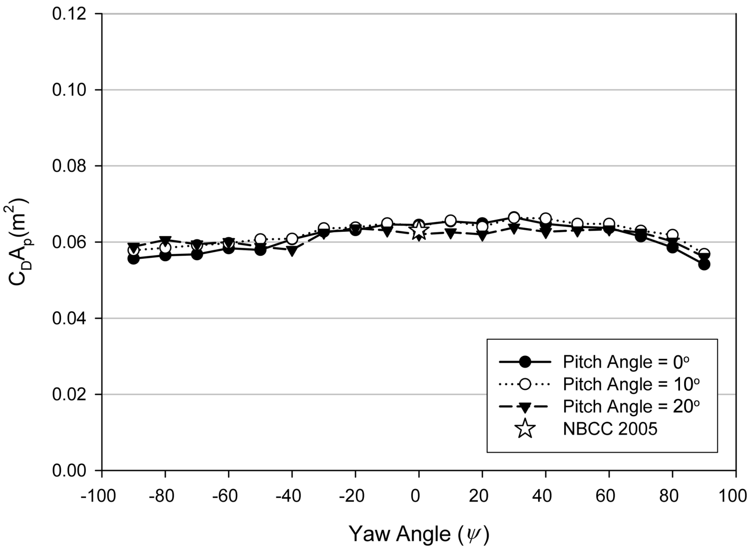

Fig. 8 Combined drag coefficient and projected frontal area, C_DA_p, vs. yaw angle for different pitch angles – Model B

the lower solidity ratio of Model B compared to Model A, as well as the symmetrical geometry of the section. This is encouraging for existing designs, as the square cross-section design is very common and has not been found to exhibit different aerodynamic behaviour under non-horizontal winds. The NBCC (2005) value for Model B matched well, and this is attributed to the symmetric geometry. It should be noted that C_DA_p at a yaw angle of 0° is higher due to the difference in the solidity ratio of the faces. The experimental data were slightly asymmetric for the two sides of the

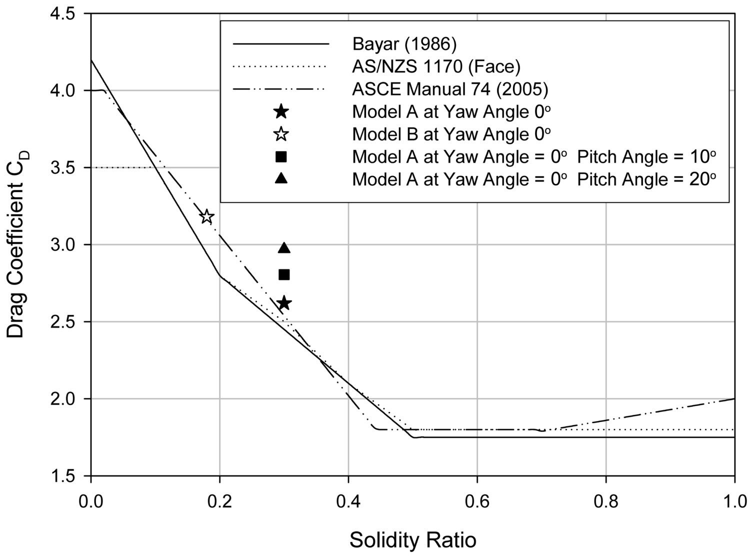

Fig. 9 Empirical and code drag coefficients for general lattice sections as a function of solidity ratio

tower, however this change is believed to reflect small variations in the wind flow field in the order of 3%.

Fig. 9 shows the drag coefficients of Models A and B plotted against code specified and empirical values. It can be seen that at a yaw angle of 0°, the values match well to those predicted by the ASCE Manual No. 74 (1991), and are reasonable when considering the Australian/New Zealand Standard (2002) and Bayar's (1986) results. However, when the drag coefficient is calculated using the frontal area, as specified in most design codes, then there is a noticeable increase when pitch is introduced.

3.4 Discussion

Based on the experimental data, it is apparent that inclined winds about the pitch and yaw axes affect the aerodynamic behaviour of lattice sections. This was more acute for Model A than Model B, and was attributed to the non-uniform geometry of the section. The aerodynamic drag and lift ultimately translate into longitudinal and transverse forces which must be resisted by the structure. However, provisions for the increased loading posed by vertical winds are absent from all current wind design codes.

Although an empirical relationship has not been drawn between Models A and B, due to their very different geometry, the following recommendations are offered for the purpose of considering inclined winds in lattice design.

1. For lattice sections with similar faces about the vertical axis and low solidity ratios (<20%), each reviewed code contains provisions for 3-dimensional frames. An increase in loading was not apparent during any of the investigations of this type of model, and therefore no increase in loading resulting from the section aerodynamics is proposed.
2. For lattice sections with very different faces about the vertical axis and relatively high solidity ratios (>20%), none of the reviewed codes contain design provisions. An increase in loading

was observed in each investigation of this type of geometric section and is most likely due to the increase in projected area as the section becomes inclined with respect to the wind. A factor compensating for the increased drag force should be included in design procedures, which should be geometry specific. For line systems involving many structures of similar design, a static wind tunnel test of a model over a range of 30° pitch (0° to 30°) and approximately +/-50° yaw (with 0° corresponding to the face with the greatest projected area) would indicate whether measures against inclined winds should be investigated. Nevertheless, based on the experimental results, an increase of 10% to 15% in the total drag load for sections with solidity ratios in the 30% range is suggested to account for aerodynamic loading increases.

4. Application of results to wind loading codes

4.1 Structural loading and wind field vertical component factor C_{dir1}

According to the CFD simulation used for the selection of experimental pitch angles, the maximum horizontal velocity occurs in the height range of interest immediately before downburst touchdown (Kim and Hangan 2007). For typical downburst events with a diameter of approximately 1000 m, the height of maximum horizontal velocity would be around 30 m above the ground (Hangan *et al.* 2003). The maximum corresponding vertical velocity takes place directly after downburst touchdown in the simulation, and can therefore be considered to be simultaneous with the maximum horizontal velocity. The largest horizontal wind speed and corresponding vertical component were identified to have a resultant wind velocity which is 25% greater than the horizontal outflow velocity, and act an angle in the range of 20° to the horizontal axis. Generally, the horizontal and vertical components of any wind field can be combined to yield $V_{res}(\alpha)$, where α is the angle of the wind with respect to the horizontal plane. Wind loading codes use a purely horizontal wind speed to specify loading conditions and so a relationship between the resultant wind speed and the horizontal wind speed would be worthwhile. This can simply be expressed as

$$V_{res} = V_{hor}\sqrt{C_{dir1}(\alpha)} \tag{1}$$

where $C_{dir1}(\alpha)$ is the wind field vertical factor which accounts for the angle of the wind loading, α, with respect to the horizontal structure. C_{dir1} is derived from a basic trigonometric relationship, expressed as

$$C_{dir1}(\alpha) = 1 + \tan^2\alpha \tag{2}$$

The wind field vertical component factor accounts for increased loading due to the presence of a vertical component in the wind field and is applied to the horizontal wind velocity to obtain the resultant force. As vertical components will always increase the resultant wind velocity, the application of C_{dir1} to the horizontal wind pressure will never result in decreased values. As the aerodynamic properties can vary significantly with inclined winds, the direction of the resultant becomes almost as important as its magnitude for certain section geometries. Values of C_{dir1} are shown for the wind angles of interest in Table 2.

Table 2 Vertical wind factors for Models A and B

	$C_{dir1}(\alpha)$	$C_{dir2}(\theta)$		$C_{DIR}(\theta)$	
θ,α	Models A & B	Model A	Model B	Model A	Model B
0°	1.00	1.00	1.00	1.00	1.00
2°	1.00	1.00	1.00	1.00	1.00
4°	1.00	1.00	1.00	1.00	1.00
6°	1.01	1.00	1.00	1.01	1.01
8°	1.02	1.00	1.00	1.02	1.02
10°	1.03	1.04	1.00	1.07	1.03
12°	1.04	1.06	1.00	1.11	1.05
14°	1.06	1.09	1.00	1.16	1.06
16°	1.08	1.13	1.00	1.22	1.08
18°	1.10	1.13	1.00	1.25	1.11
20°	1.13	1.14	1.00	1.29	1.13

4.2 Section aerodynamic factor C_{dir2}

Differences in wind loading due to variation of the yaw angle are recognized by many codes, yet differences due to the pitch angle are not considered. In the experimental data presented, it was shown that increased loads can occur. A convenient method of accounting for the increased drag force resulting from variation of aerodynamic properties when experiencing inclined wind flow is by use of a factor. This factor is easily written as a ratio of the EPA at an arbitrary pitch angle, ($C_DA_p(\theta)$), to the EPA at the nominal pitch angle of 0°, $(C_DA_p)_{\theta=0^\circ}$, and can be applied to traditional load calculations. This is expressed as

$$C_{dir2} = \frac{C_DA_p(\theta)}{(C_DA_p)_{\theta=0^\circ}} \tag{3}$$

where θ is the pitch angle of the section with respect to the horizontal axis. This factor can be used to modify the value of the drag force, based on the angle of the wind striking the structure. Due to the fact that the structure will not always be exposed to winds possessing an inclined resultant, any value of C_{dir2} which is less than unity should not be used. Experimental values of C_{dir2} are shown for the pitch angles of interest in Table 2.

The selection of values to use for C_{dir2} is considerably more involved than C_{dir1}, as the aerodynamic behaviour can vary significantly with only a slight change in wind direction. However, values of $C_DA_p(\theta)$ can be obtained from basic wind tunnel tests fairly easily. For asymmetric or unique geometries, a relatively small series of wind tunnel tests involving varying degrees of pitch at limited yaw angles could identify whether C_{dir2} should be considered for a particular design. This increase has been shown to be in the range of 10% to 15% for a section with approximately 30% solidity for winds with a resultant at an angle of 10° to 20° to the horizontal.

4.3 Vertical wind factor C_{DIR}

Two factors that contribute to an increase in structural loading of lattice structures are a wind field

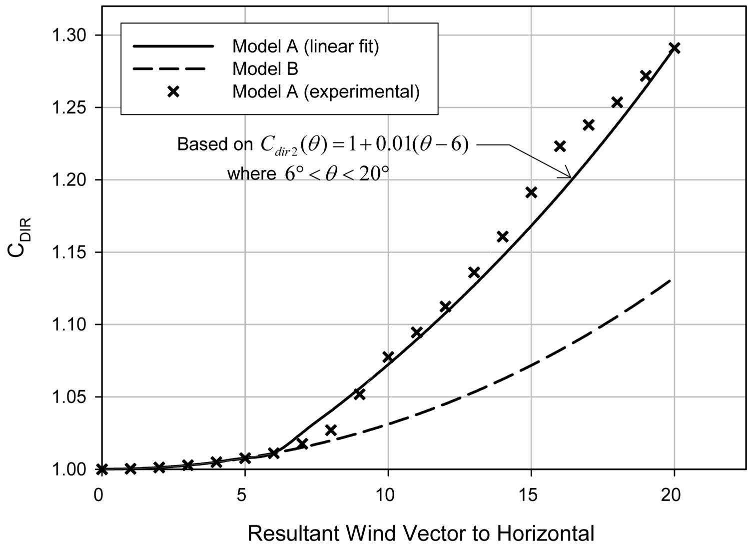

Fig. 10 Vertical wind factors for Models A (cross arm) and B (main tower section)

vertical component factor, $C_{dir1}(\alpha)$(Eq. (2)), and a section aerodynamic factor, $C_{dir2}(\theta)$(Eq. (3)). These factors are an appropriate method of accounting for the increase in wind speed due to thunderstorm gust front outflow, as well as the varying aerodynamic properties of lattice sections to inclined winds.

In order to obtain an overall vertical wind factor that includes both of the contributions, a comparison of wind direction axes to body axes is necessary. As both the inclination of the wind and the pitch of the sections are with respect to the horizontal, the angular values can be equated (e.g., $\alpha = \theta$). This allows the expression, in terms of the angle at which the resultant wind vector is coming into contact with the structure

$$C_{DIR}(\theta) = C_{dir1}(\theta) \cdot C_{dir2}(\theta) \tag{4}$$

where C_{DIR} is the vertical wind factor. As mentioned, any value of C_{dir2} which is less than unity should not be used. The values of C_{DIR} resulting from the experimental testing are shown in Table 2, and are plotted along with the linear fit for C_{dir2} of Model A in Fig. 10. Note that the values of C_{dir2} for Model B have been constrained to 1.0 for the calculation of C_{DIR}.

The vertical wind factor can be applied directly in the calculation of forces, such that

$$F_D = \frac{1}{2}\rho C_D A_p V_{hor}^2 C_{DIR}(\theta) \tag{5}$$

where ρ is air density and A_p and C_D are the drag coefficient and projected frontal area of the section at $\theta = 0°$, and V_{hor} is the horizontal design wind speed.

As shown in Table 2, the calculated drag force for a lattice section similar to Model A could be increased by as much as 29% with the inclusion of the vertical wind factor. It should be noted that for small values of θ, the increase is relatively minor. However, once an angle of 6° is reached, the factor increases rapidly. For a section similar to Model B, the only increase seen is due to the wind field vertical component factor C_{dir1}.

4.4 Inclusion in wind loading provisions

The majority of wind loading codes currently in use throughout the world have two significant limitations: firstly, vertical wind loading situations, such as those caused by thunderstorm gust fronts or downbursts, are not considered; and secondly, each code examined only includes provisions for lattice frames which have faces similar in geometry about the vertical axis of the structure (Model B). Although the majority of geometries present in many lattice structures have faces similar in geometry about the vertical axis, namely the vertical tower portions, a significant amount of structural area can frequently be found in the conductor and guy support cross arms, which are located in the upper portion of the tower. An allowance in wind code provisions for the inclusion of loading caused by inclined winds, in a fashion similar to those presented here, would allow for a greater margin of safety in structural design.

5. Conclusions

The design of a testing rig with the capability of rotating a section model about multiple body axes afforded the examination of the aerodynamic behaviour of two types of tower section models under the action of wind vectors with different pitch and yaw angles. The models used represented the conductor support cross-arm, Model A, and a typical vertical tower section, Model B, of a Manitoba Hydro HVDC Type A guyed tower. It was shown that for Model A, which has a relatively high solidity ratio, the resultant drag force tended to increase with pitch angle. This was attributed to the exposure of downwind members that may have been shielded when the model was at a pitch angle of 0^o. The increase was the most severe for yaw angles where the most frontal area was exposed, which tends to be the design case for lattice structures under convective wind events. The wind loads on Model A were approximately 14% greater for winds at a pitch angle of 20^o compared to those at a pitch angle of 0^o.

Model B, which has a relatively low solidity ratio, was not sensitive to deviations in pitch angle. In fact, the rotation about the pitch axis tended to slightly lower the drag forces on the model, as the tower became slightly more aerodynamic. The reasoning used for Model A holds; as there are less members and shielding effects, variations in pitch angle will not exhibit the significant increase in projected area and exposed members which were observed with Model A.

Failure of transmission towers due to thunderstorm wind events has been recognized as a problem by many electricity distribution companies. Many thunderstorm wind events are characterized by wind vectors possessing a substantial vertical component. Although code-specified loading coefficients provide an accurate description of the drag on rectangular and triangular cross-sections, they are typically limited in their applicability to lattice sections with different face geometry about the vertical axis, such as a support cross-arm. Current lattice design codes recognize the variation in drag with yaw angle, but lack similar provisions for deviations in pitch angle. A vertical wind factor which accounts for this should be applied to some lattice sections, depending on the geometry. Codification of these factors will most likely be reserved until full-scale observation of thuderstorm gust front and downburst outflow is better documented. However, based on the CFD simulation and experimental wind tunnel tests presented here, an approach to an overall vertical wind factor to account for increases in loads due to non-horizontal winds is proposed.

Acknowledgements

The authors would like to thank Manitoba Hydro, the Natural Sciences and Engineering Research Council of Canada (NSERC), CEA Technologies Inc. (CEATI), and the Institute for Catastrophic Loss Reduction (ICLR) for providing financial support for this project. Acknowledgment and thanks are also extended to the technical staff of the Boundary Layer Wind Tunnel Laboratory for assisting various portions of the experimental phases of the study. The input of Dr. T.C.E. Ho is also gratefully acknowledged.

References

American Society of Civil Engineers (ASCE) (1991), *Guidelines for electrical transmission line structural loading*, ASCE Manuals and Reports on Engineering Practice, No. 74, New York, USA.

American National Standards Institute (1982), *Minimum Design Loads for Buildings and Other Structures*, ANSI Standard A58.1-1982, New York, USA.

ANSI/TIA (2006), *Structural Standard for Antenna Supporting Structures and Antennas*, ANSI Standard TIA-222-G, Telecommunications Industry Association, Arlington, VA, USA.

Bayar, D.C. (1986), "Drag coefficients of lattice structures", *J. Struct. Eng.-ASCE*, **112**(2), 417-430.

British Standards Institution (1972), *British Standard Code of Practice CP3: Code of Basic Data for the Design of Buildings, Chapter V: Loading: Part 2: Wind loads*, London, UK.

Carril Jr., C.F., Isyumov, N. and Brasil, R.M.L.R.F. (2003), "Experimental study of the wind forces on rectangular latticed communication towers with antennas", *J. Wind Eng. Ind. Aerod.,* **91**(8), 1007-1022.

Chay, M.T., Albermani, F. and Wilson, R. (2006), "Numerical and analytical simulation of downburst wind loads", *Eng. Struct*., **28**(2), 240-254.

Chen, L. and Letchford, C.W. (2004), "Parametric study on the along-wind response of the CAARC building to downbursts in the time domain", *J. Wind Eng. Ind. Aerod.*, **92**(9), 703-724.

Dempsey, D. and White, H.B. (1996), "The cause of most transmission structure outages in the world is high intensity winds", *T&D World Mag.*, **48**(6), 32-42.

Flachsbart, O. (1932), "Winddruck auf vollwandige bauwerke und gitterfachwerke", *Int. Assoc. Bridge Struct. Eng.*, **1**, 153-172.

Flachsbart, O. and Winter, H. (1934), "Modellversuche ueber die belastung von Gitterfachwerken durch Windkrafte", *Der Stahblau*, Translated by Scandia Corporation, Report No. AFSWP-464.

Fujita, T.T. (1985), *The Downburst: Microburst and Macroburst*, SMRP Research Paper 210, Department of Geophysical Sciences, University of Chicago.

Fujita, T.T. (1990), "Downbursts: Meteorological features and wind field characteristics", *J. Wind Eng. Ind. Aerod.,* **36**(1), 75-86.

Georgiou, P.N. and Vickery, B.J. (1979), "Wind loads on building frames", *Proceedings of the 5th International Conference of Wind Engineering*, Fort Collins, CO, USA, July.

Hangan, H.M., Roberts, D., Xu, Z. and Kim, J. (2003), "Downburst simulations. Experimental and numerical challenges", *Proceedings of the 11th International Conference on Wind Engineering*, Lubbock, TX, USA, June.

Holmes, J.D. and Oliver, S.E. (2000), "An empirical model of a downburst", *Eng. Struct*., **22**(9), 1167-1172.

Holmes, J.D., Hangan, H.M., Schroeder, J.L., Letchford, C.W. and Orwig, K.D. (2008), "A forensic study of the Lubbock-Reese downdraft of 2002", *Wind Struct*., **11**(2), 137-152.

Jacobs, B.E.A. (1978), "Determination of shielding factors for multiple frame structures", *Proceedings of the 3rd Colloquium on Wind Engineering*, Aachen, Germany.

Kim, J. and Hangan, H.M. (2007), "Numerical simulation of impinging jets with application to downbursts", *J. Wind Eng. Ind. Aerod.*, **95**(4), 279-298.

Kim, J., Hangan, H.M. and Ho, T.C.E. (2007), "Downburst versus boundary layer induced wind loads for tall buildings", *Wind Struct*., **10**(5), 481-494.

Letchford, C.W., Mans, C. and Chay, M.T. (2002), "Thunderstorms – their importance in wind engineering (a case for the next generation wind tunnel)", *J. Wind Eng. Ind. Aerod.,* **90**(12-15), 1415-1433.

Li, C.Q. (2000), "A stochastic model of severe thunderstorms for transmission line design", *Probabilist. Eng. Mech.*, **15**(4), 359-364.

Lin, W.E., Orf, L.G., Savory, E. and Novacco, C. (2007), "Proposed large-scale modelling of the transient features of a downburst outflow", *Wind Struct.,* **10**(4), 315-346.

Mason, M.S., Wood, G.S. and Fletcher, D.F. (2009), "Influence of tilt and surface roughness on the outflow wind field of an impinging jet", *Wind Struct*., **12**(3), 179-204.

McCarthy, P. and Melsness, M. (1996), *Severe weather elements associated with September 5th, 1996 hydro tower failures near Grosse Isle, Manitoba, Canada*, Manitoba Environmental Services Centre, Environment Canada.

National Research Council Canada (1977), *National Building Code of Canada 1977*, Canadian Commission on Building and Fire Codes.

National Research Council Canada (2005), *National Building Code of Canada 2005*, Canadian Commission on Building and Fire Codes.

Nolasco, J.F. (1996), *Analysis of recent transmission line failures*, CIGRÉ WG 22.06: Review of IEC 826: Loading and Strength of Overhead Lines, CIGRÉ, 87-98.

Oliver, S.E., Moriarty, W.W. and Holmes, J.D. (2000), "A risk model for design of transmission line systems against thunderstorm downburst winds", *Eng. Struct*., **22**(9), 1173-1179.

Orwig, K.D. and Schroeder, J.L. (2007), "Near-surface wind characteristics of extreme thunderstorm outflows", *J. Wind Eng. Ind. Aerod.,* **95**(7), 565-584.

Pagon, W.W. (1958), "Wind forces on structures-plate girders and trusses", *J. Struct. Div.-ASCE*, **84**(ST-4), 1711-1-1711-27.

Ponte Jr., J. and Riera, J.D. (2007), "Wind velocity field during thunderstorms", *Wind Struct*., **10**(3), 287-300.

Savory, E., Hangan, H.M., El Damatty, A.A., Galsworthy, J. and Miller, C. (2008), "Modeling and prediction of failure of transmission lines due to high intensity winds", *Proceedings of the 2008 ASCE Structures Congress*, Vancouver, BC, Canada, April.

Savory, E., Parke, G.A.R., Zeinoddini, M., Toy, N. and Disney, P. (2001), "Modelling of tornado and microburst-induced wind loading and failure of a lattice transmission tower", *Eng. Struct.*, **23**(4), 365-375.

Shehata, A.Y. and El Damatty, A.A. (2007), "Behaviour of guyed transmission line structures under downburst wind loading", *Wind Struct*., **10**(3), 249-268.

Shehata, A.Y. and El Damatty, A.A. (2008), "Failure analysis of a transmission tower during a microburst", *Wind Struct*., **11**(3), 193-208.

Standards Australia (2002), *Structural design actions. Part 2: Wind actions. Australian/New Zealand Standard*, AS/NZS 1170.2:2002.

Standards Australia (2003), *Guidelines for design and maintenance of overhead lines C(b)1-2003*, Electrical Supply Association of Australia.

Sykes, D.M. (1981), "Lattice frames in turbulent airflow", *J. Wind Eng. Ind. Aerod.,* **7**(2), 203-214.

Whitbread, R.E. (1979), "The influence of shielding on the wind forces experienced by arrays of lattice frames", *Proceedings of the 5th International Conference on Wind Engineering*, Fort Collins, CO, USA, July.

Wood, G.S., Kwok, K.C.S., Motteram, N.A. and Fletcher, D.F. (2001), "Physical and numerical modelling of thunderstorm downbursts", *J. Wind Eng. Ind. Aerod.,* **89**(6), 535-552.

JH

Nomenclature

A_p	Projected frontal area for normal wind
C_D	Drag coefficient
$C_{dir1}(\alpha)$	Wind field vertical component factor (at angle α to horizontal)
$C_{dir2}(\theta)$	Section aerodynamic factor (at angle θ to horizontal)
$C_{DIR}(\theta)$	Vertical wind factor (at angle θ to horizontal)
F_D	Drag force
V_{hor}	Gust front horizontal wind velocity
V_{ver}	Gust front vertical wind velocity
$V_{RES}(\theta)$	Gust front resultant wind velocity (at angle θ to horizontal)
α	Angle of resultant wind velocity to the horizontal
ρ	Air density
θ	Pitch angle of structure to the horizontal
ψ	Yaw angle (azimuth)